Synthesis and Characterization of a New Polymorph of PtI Containing an Ordered MX Chain

Brian Scott, Bobby L. Bracewell, Sabina R. Johnson, and Basil I. Swanson

Los Alamos National Laboratory
Spectroscopy and Biochemistry Group (CST-14)
Los Alamos, New Mexico, 87545

J. F. Bardeau and A. Bulou

Lab PEC, Université du Maine
72017 Le Mans cedex, France

B. Hennion

LLB, CEN Saclay
91191 Gif/Yvette cedex, France

Received August 17, 1995
Revised Manuscript Received December 19, 1995

Introduction

We wish to report a new structural modification of $[Pt(en)_2I_2][Pt(en)](ClO_4)_4$ (PtI/en/ClO_4) that was discovered while studying fully deuterated PtI/en/ClO_4 (D-PtI/en/ClO_4) samples (en = 1,2-diaminoethane). The first evidence that the deuterated form had a different structure came from neutron diffraction experiments,[1] which revealed a doubling of two of the cell constants from the protonated structure (H-PtI/en/ClO_4).[2] A subsequent X-ray diffraction study gave the full molecular and crystal structure. The most significant feature of the new structure is the presence of an ordered MX chain sublattice; the doubling of the unit cell along two unit-cell directions results in two crystallographically distinct MX chains. (MX chain refers to the X−Pt−X- -Pt- -X backbone.) One of these chains is similar in charge density wave (CDW) strength to that observed in the H-PtI/en/ClO_4 structure, and forms a sublattice of disordered chains. The other chain is a weaker CDW and forms a sublattice of ordered MX chains. Additional investigation of several samples showed that all D-PtI/en/ClO_4 crystals had the new structure but that a few H-PtI/en/ClO_4 crystals also had the new structure. The new structural result will be presented along with a brief description of the resonance Raman results. A discussion of this polymorphism in terms of hydrogen bonding and crystal growth conditions will be presented herein.

Examples of deuteration induced phase transitions exist in the literature. Cytochrome *c* oxidase[3] and the transition-metal complex bis(3-amino-3-methyl-2-butanone oximato)nickel(II) chloride monohydrate,[4] $[Ni(ao)_2\text{-}H]^+Cl^-\cdot H_2O$, are two systems that undergo structural changes as a result of H−D exchange. In cytochrome *c* oxidase resonance Raman spectroscopy shows that the porphyrine/heme pocket structure is changed upon deuterium exchange. The shifts are in side chains on the heme pocket and are attributed to a weakening in hydrogen bonding between these side chains and surrounding amino acid residues brought on by deuterium exchange. While this structural change in cytochrome *c* is subtle, the change in $[Ni(ao)_2\text{-}H]^+Cl^-\cdot H_2O$ is striking. The crystal structure changes from space group $P2_1/c$ to $P2_1$ upon deuteration and is accompanied by significant changes in the hydrogen bonding between complexes. This hydrogen bonding is weakened upon deuteration and is typical upon D for H substitution. We will show in our system that the deuterium bonds are actually shorter than the hydrogen bonds. It is in this unique feature that lies the explanation for the polymorphism in PtI/en/ClO_4.

The new polymorph of PtI/en/ClO_4 is the first case of an MX material with a three-dimensionally ordered chain lattice. All MX materials studied to date contain disordered chain lattices.[5] Even though each MX chain is one-dimensionally ordered, the random packing of MX chains in the crystal causes a three-dimensional disorder. This disorder is observed as two halide peaks in the bridging region. One class of MX materials, PtX/chxn/X, are known to be ordered in two dimensions, but disorder in the third dimension causes the classic disordered bridging region.[6] We will show that in the new phase of PtI/en/ClO_4 every other chain is ordered, producing a three-dimensionally ordered sublattice in which only one halide is observed in the bridging region. This presents a unique opportunity to study the interchain interactions that might lead to a fully ordered MX system and the behavior of ordered versus disordered chain systems. This system also has interesting ramifications for the "template effect", which states that a unique counterion−ligand template imposes a unique CDW strength on the MX chain.[7] The presence of two chains of different CDW strength in the same counterion−ligand template necessitates another look at this model that all other MX materials obey.

Experimental Section

Synthesis.[8] H-PtI/en/ClO_4 and D-PtI/en/ClO_4 were synthesized as described previously in the literature. In the case of D-PtI/en/ClO_4 (en = $H_2NCD_2CD_2NH_2$) was used as obtained from Cambridge isotopes and the crystals were crystallized from D_2O in a sealed system by slowly decreasing the temperature from 40 to 30 °C.

X-ray.[9] A rectangular, slab-shaped crystal of D-PtI/en/ClO_4, with dimensions of 0.08 × 0.18 × 0.21 mm^3 was mounted for data collection. The crystal was indexed as monoclinic C with

(1) Bardeau, J. F.; Swanson, B. I.; Hennion, B.; Bulou, A. Journées de la neutronique, cap d'Agde, May 1994.

(2) The structure of H-PtI/en/ClO_4 was originally reported by two groups in 1979; one group reported the structure in acentric space group *C*2,[17] while the other reported centric space group *C*2/*m*.[18] We have since confirmed the latter determination by Keller et al.[18]

(3) Hildebrandt, P.; Vanhecke, F.; Heibel, G.; Mauk, A. G. *Biochemistry* **1993**, *32*, 14158.

(4) Hsu, B.; Schlemper, E. O.; Fair, C. K. *Acta Crystallogr.* **1980**, *B36*, 1387.

(5) Huckett, S. C.; Scott, B.; Love, S. P.; Donohoe, R. J.; Burns, C. J.; Garcia, E.; Frankcom, T.; Swanson, B. I. *Inorg. Chem.* **1993**, *32*, 2137.

(6) Hazell, A. *Acta Crystallogr.* **1991**, *C47*, 962.

(7) Scott, B.; Love, S. P.; Kanner, G. S.; Johnson, S. R.; Wilkerson, M. P.; Berkey, M.; Swanson, B. I.; Saxena, A.; Huang, X. Z.; Bishop, A. R. *J. Mol. Struct.* **1995**, *356*, 207.

(8) Huckett, S. C.; Donohoe, R. J.; Worl, L. A.; Bulou, A. D. F.; Burns, C. J.; Laia, J. R.; Carroll, D.; Swanson, B. I. *Chem. Mater.* **1991**, *3*, 123.

(9) Lattice determination and data collection were carried out using XSCANS Version 2.10b software. All data reduction, including Lorentz and polarization corrections and structure solution, refinement, and graphics were performed using SHELXTL PC Version 4.2/360 software. XSCANS and SHELXTL PC are products of Siemens Analytical X-ray Instruments, Inc., 6300 Enterprise Lane, Madison, WI 53719. $R_1 = \sum||F_o| - |F_c||/\sum|F_o|$ and $R_{2w} = [\sum[w(F_o^2 - F_c^2)^2]/\sum[w(F_o^2)^2]]^{1/2}$. The parameter $w = 1/[\sigma^2(F_o^2) + (0.0579P)^2 + 168.5856P]$.

0897-4756/96/2808-0321$12.00/0

Table 1. Atomic Coordinates ($\times 10^4$) and Equivalent Isotropic Thermal Parameters ($Å^2 \times 10^3$) for Deuterated PtI/en/ClO_4

atom	*x*	*y*	*z*	*U*(eq)[a]
Pt(1)	0	0	0	15(1)
Pt(2)	0	5000	0	16(1)
Pt(3)	2500	2500	0	16(1)
I(1)	0	2360(2)	0	27(1)
I(2)	2499(1)	200(4)	5(4)	24(2)
Cl(1)	3202(4)	0	4713(16)	38(3)
Cl(2)	1793(4)	0	5260(15)	36(3)
Cl(3)	704(3)	2487(4)	4749(13)	37(2)
O(1)	2954(8)	1003(16)	4638(30)	55(7)
O(2)	3468(14)	0	6272(60)	92(16)
O(3)	3411(11)	0	3266(53)	72(12)
O(4)	2038(7)	1014(15)	5391(27)	42(6)
O(5)	1527(14)	0	3654(57)	90(16)
O(6)	1565(11)	0	6762(51)	70(11)
O(7)	452(8)	1474(16)	4622(28)	52(6)
O(8)	469(7)	3490(15)	4604(26)	46(6)
O(9)	979(13)	2493(15)	6439(42)	101(15)
O(10)	920(9)	2445(13)	3184(40)	60(8)
N(1)	293(10)	0	−2258(41)	24(5)
N(2)	572(10)	0	1389(42)	24(5)
N(3)	280(10)	5000	−2270(39)	23(5)
N(4)	586(10)	5000	1350(40)	23(5)
N(5)	2221(7)	2511(12)	2275(33)	24(5)
N(6)	1921(8)	2489(11)	−1368(38)	27(5)
C(1)	720(17)	227(48)	−1849(71)	49(14)
C(2)	898(16)	206(52)	161(69)	49(14)
C(3)	722(14)	5188(44)	−1845(58)	33(11)
C(4)	881(16)	4695(33)	39(68)	33(11)
C(5)	1762(12)	2222(31)	1614(53)	15(5)
C(5′)	1773(12)	2821(32)	1586(52)	15(5)
C(6)	1675(12)	2219(31)	−119(52)	15(5)
C(6′)	1670(12)	2867(31)	−81(51)	15(5)

[a] *U*(eq) is defined as one-third of the trace of the orthogonalized U_{ij} tensor.

lattice constants similar to H-PtI/en/ClO_4. One-hour axial photographs showed discrete reflections corresponding to a doubling of the *a* and *b* axes. (The diffuse streaking observed in the *b* axis/chain axis axial photos of H-PtI/en/ClO_4 and all other MX structures coalesced into discrete reflections.) Accurate centering gave the lattice $a = 33.828(3)$ Å, $b = 11.638(1)$ Å, $c = 7.433(1)$ Å, and $\beta = 98.490(6)°$. Reflections in the range $3° < 2\theta < 50°$ were collected on a Seimens P4/PC diffractometer with graphite-monochromatized Mo Kα radiation. Structure refinement began in space group *C*2/*m* with Pt atoms at 0 0 0; 0 ¼ ¼; 0 ½ 0. All remaining atoms appeared on subsequent Fourier maps. All en ligands were disordered and refined as two one-half occupancy ligands. Due to this disorder, hydrogen atoms were not placed on the en ligands. All atoms, except for the disordered en carbon atoms, were refined anisotropically to a final $R_1 = 0.0525$ and $R_{2w} = 0.1223$.[9] Atomic coordinates and equivalent isotropic displacement parameters are given in Table 1.

Several samples of D-PtI/en/ClO_4 and H-PtI/en/ClO_4 were mounted, indexed, and photographed. Three deuterated samples all showed the lattice corresponding to the D-PtI/en/ClO_4 structure. Two out of three H-PtI/en/ClO_4 samples showed the H-PtI/en/ClO_4 structure, while the third showed the D-PtI/en/ClO_4 structure.

Resonance Raman. Raman spectra were obtained from carefully selected single-crystal samples maintained at either 35 or 42 K by an Air Products Displex closed-cycle helium cryostat. Excitation was provided by a Ti:sapphire solid-state laser, pumped by an Ar^+ ion laser, with the polarization axis of the laser output aligned parallel to the chain axis of the samples. The wavelength of the Ti:sapphire laser was adjusted to match that at which maximum fine structure was observed in resonance Raman experiments on H-PtI/en/ClO_4 samples. The exciting radiation was incident on the bc face of the crystals and was focused to give a beam power of about 16 W/cm^2 at the sample surface. (There was no evidence that this power level caused local heating and associated crystal damage and/or production of defects.) The scattered radiation was collected in a backscattering geometry and coupled into a SPEX Model 1877D triple spectrograph equipped with a 1200 gratings/mm diffraction grating blazed for a wavelength of 900 nm. The resulting spectra were recorded using a Photometrics Incorporated PM512 prime grade charge-coupled device detector with National Instruments Corp. Lab VIEW 2 program used to perform the integrations and store the data. Calibration of both the wavelength scale for the recorded spectra and the laser wavelength were accomplished using accurately known lines from a Ne discharge lamp.

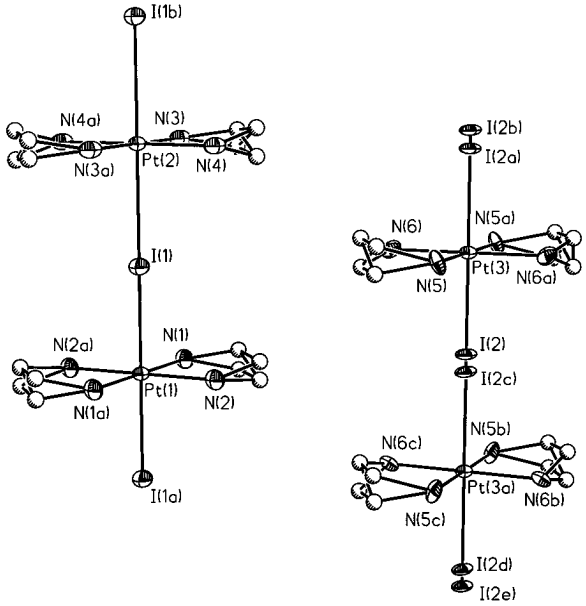

Figure 1. Plot showing the ordered and disordered chains in PtI/en/ClO_4. Carbon atoms were refined isotropically and are shown as shaded spheres.

Results and Discussion

The two independent chains of D-PtI/en/ClO_4 are shown in Figure 1. The ordered chain has Pt atoms sitting on 2/*m* symmetry sites, with the bridging iodide atoms on 2-fold axes coincident with the chain axis. Each Pt site may be identified as either Pt^{2+} or Pt^{4+} based on the bond lengths to the bridging iodide. The CDW strength of this ordered chain is weak; the short Pt^{4+}−I distance is 2.747(2) Å and the long Pt^{2+}- -I distance is 3.072(1) Å resulting in $\rho = 0.894(1)$. (ρ is the ratio of the short Pt−I bond length to the long Pt- -I bond length.) The disordered chains in the unit cell have Pt atoms sitting on inversion centers. There is a mirror plane sitting halfway between these Pt atoms and two half-occupancy iodide atoms are observed; the oxidation states of the Pt sites cannot be identified due to this disorder. The short and long bonds are 2.677(4) and 3.142(4) Å, respectively. This yields $\rho = 0.852(2)$, a value close to the $\rho = 0.868(1)$ of our version of the H-PtI/en/ClO_4 structure.[10]

The hydrogen bonding in the H- and D-PtI/en/ClO_4 systems is quite different. In both structures the chains are tied together along the c direction by way of N−H···O hydrogen bonds. Furthermore, this hydrogen bonding is two dimensional, with no hydrogen bonding between the chains in the *a* direction. In the deuterated form this hydrogen-bonding produces sheets of alternat-

(10) Scott, B.; Johnson, S. R.; Swanson, B. I. *Acta Crystallogr. C*, manuscript in preparation.

ing ordered and disordered chains perpendicular to the *a* axis. A well accepted criteria for hydrogen bonding is $r_{vw} - r_{ex} \geq -0.2$, where r_{vw} = the sum of van der Waals radii for N and O and r_{ex} = the experimental N···O contact.[11] In H-PtI/en/ClO_4 there are two N···O contacts of 3.317 and 3.304 Å in length, and the sum of the van der Waals radii for N and O is 3.05 Å. The average difference of $r_{vw} - r_{ex}$ is −0.25 Å. Thus, according to this criteria, the hydrogen bonding in H-PtI/en/ClO_4 is absent. (We feel that there must be some hydrogen bonding here in order to stabilize the crystal lattice, but that it is extremely weak.) In contrast, the D-PtI/en/ClO_4 structure has N···O contacts ranging from 3.003 to 3.207 Å. This gives a $r_{vw} - r_{ex}$ range of −0.1 to 0, indicating that the hydrogen bonding in D-PtI/en/ClO_4 is significantly stronger than in PtI/en/ClO_4. This strengthening of the hydrogen bonding is not normally observed upon deuteration,[3,4] and we feel that a minimization of lattice energy through hydrogen bonding is responsible for this behavior.

This optimization in hydrogen bonding is probably the driving force behind the polymorphism in PtI/en/ClO_4. This explanation is supported by the predominant occurrence of the new structure in deuterated samples. It is known that hydrogen bonding is responsible for the phase transitions observed in PtCl/en/ClO_4 and PtBr/en/ClO_4.[5,12] As the temperature is raised in these systems, hydrogen bonding is weakened by increased thermal motion in the perchlorate ions. This results in a reorganization of the hydrogen bonding network in order to minimize crystal lattice energy. We propose a similar mechanism as an explanation for the polymorphism in PtI/en/ClO_4. The major difference is that the hydrogen bonding is weakened by deuterium substitution instead of temperature. The hydrogen bonding in H-PtI/en/ClO_4 is already very weak (vide supra). If the D-PtI/en/ClO_4 material were to take on the H-PtI/en/ClO_4 structure, the hydrogen bonding would be even weaker, perhaps nonexistent. Therefore, in order to form a stable crystal a new structure is formed that maximizes the hydrogen bonding through the formation of shorter N···O contacts. The presence of the D-PtI/en/ClO_4 structure among a few samples of H-PtI/en/ClO_4 must, however, be explained. We believe that the H-PtI/en/ClO_4 structure is very close to the D-PtI/en/ClO_4 structure and that crystallization conditions such as concentration, temperature, rate of crystal formation, etc., are all critical parameters in determining the phase of a given PtI/en/ClO_4 crystal. We are presently carrying out controlled crystallization experiments to discover these conditions. Finally, Yamashita et al. have mentioned polymorphism in PtBr/en/ClO_4; they have discovered two room temperatures structures in space groups $C2/m$ and $P2_1/m$ as well as different ν_1 frequencies for these two structures.[13] These crystals also have weak hydrogen bonding with a $r_{vw} - r_{ex}$ of −0.10. Not much has been published on either of these structures, but they give precedence for polymorphism in MX chains.

The I−Pt−I stretching frequency band has more structure in H- and D-PtI/en/ClO_4 samples that have the new structure. We are presently performing additional resonance Raman studies to ascertain the nature of the additional Raman structure.

Conclusion

The new polymorph of PtI/en/ClO_4 is of interest on many different fronts. The magnetic, electrical, and optical properties of the new structural modification are likely to vary on a molecular scale; the two chains of different CDW strength will have different physical properties. It is well-known that nanoscale magnetic and electronic systems, such as nanostructural magnetic layers created by molecular beam epitaxy, have properties different from those of the bulk magnetic material.[14] These magnetic studies are presently underway. The disordered and ordered sublattices of MX chains present an opportunity to study effects of T, P, and chemical doping on ordered versus disordered chains. The polymorphism in this system is linked to a different hydrogen bonding network, with the MX chains being slightly perturbed from the normal PtI structure. This type of polymorphism is often observed in protein structures, especially in peptide structures having 8−20 amino acid residues.[15] Studies of such polymorphism is interesting in the spirit of molecular recognition and materials engineering.[16]

Acknowledgment. This work was supported by the Office of Basic Energy Sciences, Division of Materials Science of the DOE, and the Center for Materials Science at LANL.

Supporting Information Available: Tables of crystal data (8 pages); table of observed and calculated structure factors (6 pages). Ordering information is given on any current masthead page.

CM9503893

(11) Pimentel, G. C.; McClellan, A. L. In *The Hydrogen Bond*; 1960, W. H. Freeman and Co.: San Francisco, 1960; p 255.
(12) Toriumi, K.; Yamashita, M.; Kurita, S.; Murase, I.; Ito, T. *Acta Crystallogr.* **1993**, *B49*, 497.
(13) Yamashita, M. personal communication, 1994.
(14) Grundy, P. J.; Greig, D.; Hill, E. W. *Endeavour* **1993**, *17*, 154.
(15) Karle, I. L. *Acta Crystallogr.* **1992**, *B48*, 341.
(16) McBride, J. M.; Kahr, B. *Angew. Chem., Int. Ed. Engl.* **1992**, *31*, 1.
(17) Matsumoto, N.; Yamashita, M.; Kida, S.; Ueda, I. *Acta Crystallogr.* **1979**, *B35*, 1458.
(18) Endres, H.; Keller, H. J.; Martin, R.; Gung, H. N.; Traeger, U. *Acta Crystallogr.* **1979**, *B35*, 1885.